

The World-Trade Web: Topological Properties, Dynamics, and Evolution

Giorgio Fagiolo, Javier Reyes, Stefano Schiavo

▶ **To cite this version:**

Giorgio Fagiolo, Javier Reyes, Stefano Schiavo. The World-Trade Web: Topological Properties, Dynamics, and Evolution. 2008. hal-01066180

HAL Id: hal-01066180

https://sciencespo.hal.science/hal-01066180

Preprint submitted on 19 Sep 2014

HAL is a multi-disciplinary open access archive for the deposit and dissemination of scientific research documents, whether they are published or not. The documents may come from teaching and research institutions in France or abroad, or from public or private research centers.

L'archive ouverte pluridisciplinaire **HAL**, est destinée au dépôt et à la diffusion de documents scientifiques de niveau recherche, publiés ou non, émanant des établissements d'enseignement et de recherche français ou étrangers, des laboratoires publics ou privés.



Laboratory of Economics and Management

Sant'Anna School of Advanced Studies
Piazza Martiri della Libertà, 33 - 56127 PISA (Italy)
Tel. +39-050-883-343 Fax +39-050-883-344
Email: lem@sssup.it Web Page: http://www.lem.sssup.it/

LEM

Working Paper Series

The World-Trade Web: Topological Properties, Dynamics, and Evolution

Giorgio Fagiolo[†], Javier Reyes[‡], Stefano Schiavo[*]

†Sant'Anna School of Advanced Studies, Pisa, Italy.
‡Department of Economics, Sam M. Walton College of Business, University of Arkansas, USA.
*Department of Economics and School of International Studies, University of Trento, Italy, and OFCE, France.

2008/16 **July 2008**

The World-Trade Web: Topological Properties, Dynamics, and Evolution

Giorgio Fagiolo

Sant'Anna School of Advanced Studies,

Laboratory of Economics and Management,

Piazza Martiri della Libertà 33, I-56127 Pisa,

Italy. Tel: +39-050-883356 Fax: +39-050-883343. E-mail: giorgio.fagiolo@sssup.it

Javier Reyes

Department of Economics, Sam M. Walton College of Business,

University of Arkansas, USA. E-mail: JReyes@walton.uark.edu

Stefano Schiavo

Department of Economics and School of International Studies,

University of Trento, Italy and OFCE. E-mail: stefano.schiavo@ofce.sciences-po.fr

(Dated: July 2008)

Abstract

This paper studies the statistical properties of the web of import-export relationships among world countries using a weighted-network approach. We analyze how the distributions of the most important network statistics measuring connectivity, assortativity, clustering and centrality have co-evolved over time. We show that all node-statistic distributions and their correlation structure have remained surprisingly stable in the last 20 years – and are likely to do so in the future. Conversely, the distribution of (positive) link weights is slowly moving from a log-normal density towards a power law. We also characterize the autoregressive properties of network-statistics dynamics. We find that network-statistics growth rates are well-proxied by fat-tailed densities like the Laplace or the asymmetric exponential-power. Finally, we find that all our results are reasonably robust to a few alternative, economically-meaningful, weighting schemes.

PACS numbers: 89.75.-k, 89.65.Gh, 87.23.Ge, 05.70.Ln, 05.40.-a

Keywords: Weighted Networks; World Trade Web; Distribution Dynamics; Power Laws; Econophysics.

I. INTRODUCTION

In the last decade, a lot of effort has been devoted to the empirical exploration of the architecture of the World Trade Web (WTW) from a complex-network perspective [1–12]. The WTW, also known as International Trade Network (ITN), is defined as the network of import/export relationships between world countries in a given year. Understanding the topological properties of the WTW, and their evolution over time, acquires a fundamental importance in explaining international-trade issues such as economic globalization and internationalization [13, 14]. Indeed, it is common wisdom that trade linkages are one of the most important channels of interaction between world countries [15]. For example, they can help to explain how economic policies affect foreign markets [16]; how economic shocks are transmitted among countries [17]; and how economic crises spread internationally [18]. However, direct bilateral-trade relationships can only explain a small fraction of the impact that an economic shock originating in a given country can have on another one, which is not among its direct-trade partners [19]. Therefore, a complex-network analysis [20–23] of the WTW, by characterizing in detail the topological structure of the network, can go far beyond the scope of standard international-trade indicators, which instead only account for bilateral-trade direct linkages [61].

The first stream of contributions that have studied the properties of the WTW has employed a *binary-network analysis*, where a (possibly directed) link between any two countries is either present or not according to whether the trade flow that it carries is larger than a given lower threshold [2–4]. According to these studies, the WTW turns out to be characterized by a high density and a right-skewed (but not exactly power-law) distribution for the number of partners of a given country (i.e., the node degree). Furthermore, there seems to be evidence of bimodality in the node-degree distribution. While the majority of countries entertain few trade partnerships, there exists a group of countries trading with almost everyone else [10, 12]. Also, the binary WTW is a very disassortative network (i.e., countries holding many trade partners are on average connected with countries holding few partners) and is characterized by some hierarchical arrangements (i.e., partners of well connected countries are less interconnected among them than those of poorly connected ones). Remarkably, these properties are quite stable over time [4].

More recently, a few contributions have adopted a *weighted-network approach* [24–26] to the study of the WTW, where each link is weighted by some proxy of the trade intensity that it carries. The motivation is that a binary approach cannot fully extract the wealth of information about the trade intensity flowing through each link and therefore might dramatically underestimate

the role of heterogeneity in trade linkages. Indeed, Refs. [9, 10, 12] show that the statistical properties of the WTW viewed as a weighted network crucially differ from those exhibited by its weighted counterpart. For example, the weighted version of the WTW appears to be weakly disassortative. Moreover, well-connected countries tend to trade with partners that are strongly-connected between them. Finally, the distribution of the total trade intensity carried by each country (i.e., node strength) is right-skewed, indicating that a few intense trade connections co-exist with a majority of low-intensity ones. This is confirmed, at the link level, by Refs. [6, 7] who find that the distribution of link weights can be approximated by a log-normal density robustly across the years [1]. The main insight coming from these studies is that a weighted-network analysis is able to provide a more complete and truthful picture of the WTW than a binary one [12].

Additional contributions have instead focused on specific features of the structure and dynamics of the WTW. For example, Refs. [3, 8] find evidence in favor of a hidden-variable model, according to which the topological properties of the WTW (in both the binary and weighted case) can be well explained by a single node-characteristic (i.e., country gross-domestic product) controlling for the potential ability of a node to be connected. Furthermore, Ref. [5] studies the weighted network of bilateral trade imbalances [62]. The Authors note that also the international trade-imbalance network is characterized by a high level of heterogeneity: for each country, the profile of trade fluxes is unevenly distributed across partners. At the network level, this prompts to the presence of high-flux backbones, i.e. sparse subnetworks of connected trade fluxes carrying most of the overall trade in the network. The Authors then develop a method to extract (for any significance level) the flux backbone existing among countries and links. This turns out to be extremely effective in sorting out the most relevant part of the trade-imbalance network and can be conveniently used for visualization purposes. Finally, Ref. [11] considers the formation of "trade islands", that is connected components carrying a total trade flow larger than some given thresholds. The analysis of the evolution of the WTW community structure [27] finds mixed evidence for globalization.

In this paper we present a more thorough study of the topological properties of the WTW by focusing on distribution dynamics and evolution. More specifically, following the insights of Ref. [12], we employ a weighted network approach to characterize, for the period 1981-2000, the distribution of the most important network statistics measuring node connectivity, assortativity, clustering and centrality; as well as link weights. We ask three main types of questions: (i) Have (and, if so, how) the distributional properties of these statistics (and their correlation structure)

been changing within the sample period considered? (ii) Can we make any prediction on the out-of-sample evolution of such distributions? (iii) Do the answers to the previous questions change if we play with a number of alternative, economically-meaningful weighting schemes (i.e., if we allow for different rules to weight existing links)?

The rest of the paper is organized as follows. Section II presents the data sets and defines the statistics studied in the paper. Section III introduces the main results. Finally, Section IV concludes and discusses future extensions.

II. DATA AND DEFINITIONS

We employ international-trade data provided by [28] to build a time-sequence of weighted directed networks. Our balanced panel refers to $T = 20$ years (1981-2000) and $N = 159$ countries. For each country and year, data report trade flows in current US dollars. To build adjacency and weight matrices, we followed the flow of goods. This means that rows represent exporting countries, whereas columns stand for importing countries. We define a "trade relationship" by setting the generic entry of the (binary) adjacency matrix $\tilde{a}_{ij}^t = 1$ if and only if exports from country i to country j (e_{ij}^t) are strictly positive in year t.

Following Refs. [1, 6–8], the weight of a link from i to j in year t is defined as $\tilde{w}_{ij}^t = e_{ij}^t$ [63]. Thus, the sequence of $N \times N$ adjacency and weight matrices $\{\tilde{A}^t, \tilde{W}^t\}$, $t = 1981, ..., 2000$ fully describes the within-sample dynamics of the WTW.

A preliminary statistical analysis of both binary and weighted matrices suggests that $(\tilde{A}^t, \tilde{W}^t)$ are sufficiently symmetric to justify an undirected analysis for all t. From a binary perspective, the majority of WTW links are reciprocated: on average, about 93% of countries export to partners that in turn export to them. To check more formally this evidence from a weighted perspective, we have computed the weighted symmetry index defined in Ref. [29]. The index ranges in the sample period between 0.0017 and 0.0043, signalling a strong and stable symmetry of WTW weight matrices [64]. We have therefore symmetrized the network by defining the entries of the new adjacency matrix A^t so that $a_{ij}^t = 1$ if and only if either $\tilde{a}_{ij}^t = 1$ or $\tilde{a}_{ji}^t = 1$, and zero otherwise. Accordingly, the generic entry of the new weight matrix W^t is defined as $w_{ij}^t = \frac{1}{2}(\tilde{w}_{ij}^t + \tilde{w}_{ji}^t)$. This means that the symmetrized weight of link ij is proportional to the total trade (imports plus exports) flowing through that link in a given year. Finally, in order to have $w_{ij}^t \in [0, 1]$ for all (i, j) and t, we have re-normalized all entries in W^t by their maximum value $w_*^t = max_{i,j=1}^N w_{ij}^t$.

For each $(\tilde{A}^t, \tilde{W}^t)$, we study the distributions of the following node statistics:

- *Node degree* [20, 30], defined as $ND_i^t = A_{(i)}^t \mathbf{1}$, where $A_{(i)}^t$ is the i-th row of A^t and $\mathbf{1}$ is a unary vector. ND is a measure of binary connectivity, as it counts the number of trade partners of any given node. Although we mainly focus here on a weighted-network approach, we study ND because of its natural interpretation in terms of number of trade partnerships and bilateral trade agreements.

- *Node strength* [31], defined as $NS_i^t = W_{(i)}^t \mathbf{1}$, where again $W_{(i)}^t$ is the i-th row of W^t. While ND tells us how many partners a node holds, NS is a measure of weighted connectivity, as it gives us an idea of how intense existing trade relationships of country i are.

- *Node average nearest-neighbor strength* [31], that is $ANNS_i^t = (A_{(i)}^t W^t \mathbf{1})/(A_{(i)}^t \mathbf{1})$. ANNS measures how intense are trade relationships maintained by the partners of a given node. Therefore, the correlation between ANNS and NS is a measure of network assortativity (if positive) or disassortativity (if negative). It is easy to see that ANNS boils down to average nearest-neighbor degree (ANND) if W^t is replaced by A^t.

- *Weighted clustering coefficient* [9, 32], defined as $WCC_i^t = ([W^t]^{[\frac{1}{3}]})_{ii}^3/(ND_i^t(ND_i^t - 1))$. Here Z_{ii}^3 is the i-th entry on the main diagonal of $Z \cdot Z \cdot Z$ and $Z^{[\frac{1}{3}]}$ stands for the matrix obtained from Z after raising each entry to 1/3. WCC measures how much clustered a node i is from a weighted perspective, i.e. how much intense are the linkages of trade triangles having country i as a vertex [65]. Again, replacing W^t with A^t, one obtains the standard binary clustering coefficient (BCC), which counts the fraction of triangles existing in the neighborhood of any give node [33].

- *Random-walk betweenness centrality* [34, 35], which is a measure of how much a given country is globally-central in the WTW. A node has a higher random-walk betweenness centrality (RWBC) the more it has a position of strategic significance in the overall structure of the network. In other words, RWBC is the extension of node betweenness centrality [36] to weighted networks and measures the probability that a random signal can find its way through the network and reach the target node where the links to follow are chosen with a probability proportional to their weights.

The above statistics allow one to address the study of node characteristics in terms of four dimensions: connectivity (ND and NS), assortativity (ANND and ANNS, when correlated with ND and NS), clustering (BCC and WCC) and centrality (RWBC). In what follows, we will mainly

concentrate the analysis on ND and the other weighted statistics (NS, ANNS, WCC, RWBC), but we occasionally discuss, when necessary, also the behavior of ANND and BCC.

We further explore the network-connectivity dimension by studying the time-evolution of the link-weight distribution $w^t = \{w_{ij}^t, i \neq j = 1, \ldots, N\}$. In particular, we are interested in assessing the fraction of links that are zero in a given year t and becomes positive in year $t+\tau$, $\tau = 1, 2, \ldots$ and the percentage of links that are strictly positive at t and disappear in year $t+\tau$. This allows one to keep track of trade relationships that emerge or become extinct during the sample period [66].

III. RESULTS

A. Shape, Moments, and Correlation Structure of Network Statistics

We begin by studying the shape of the distributions of node and link statistics and their dynamics within the sample period under analysis. As already found in Refs. [6, 7], link weight distributions display remarkably stable moments (see Figure 1) and are well proxied by log-normal densities in each year (cf. Figure 2 for an example). This means that the majority of trade linkages are relatively weak and coexist with few high-intensity trade partnerships. The fact that the first four moments of the distribution are fairly constant in the sample period hints to a strong persistence of trade relationships. We shall study this issue in more details below.

A similar stable pattern is detected also for the moments of the distributions of all node statistics under analysis, see Figure 3 for the case of NS distributions. To see that this applies in general for node statistics, we have computed the time average (across 19 observations) of the absolute value of 1-year growth rates of the first four interesting moments of ND, NS, ANNS, WCLUST and RWBC statistics, namely mean, standard deviation, skewness and kurtosis [67]. Table I shows that these average absolute growth-rates range in our sample between 0.0043 and 0.0615, thus indicating that the shape of these distributions seem to be quite stable over time.

But how does the shape of node- and link-statistic distributions look like? To investigate this issue we have begun by running normality tests on the logs of (positive-valued) node and link statistics. As Table II suggests [68], binary-network statistic distributions are never log-normal (i.e., their logs are never normal), whereas all weighted-network statistics but RWBC seem to be well-proxied by log-normal densities. To see why this happens, Figure 4 shows the rank-size plot of ND in 2000 (with a kernel density estimate in the inset). It is easy to see that ND exhibits

some bimodality, with the majority of countries featuring low degrees and a bunch of countries trading with almost anyone else. Figure 5 shows instead, for year 2000, how NS is nicely proxied by a log-normal distribution. This is not so for RWBC, whose distribution is instead power-law in all years, with slopes oscillating around -1.15, see Figures 6 and 7. Therefore, being more central is more likely than having high NS, ANNS, or WCC (i.e., the latter distributions feature upper tails thinner than that of RWBC distributions; we shall return to complexity issues related to this point when discussing out-of-sample evolution of the distributions of node and link statistics).

We now discuss in more detail the evolution over time of the moments of the distributions of node statistics. As already noted in Refs. [3, 6, 7, 12], the binary WTW is characterized by an extremely high network density $d^t = \frac{1}{N(N-1)} \sum_i \sum_j a_{ij}^t$, ranging from 0.5385 to 0.6441. Figure 8 plots the normalized (by N) population-average of ND, which is equal to network density up to a $N^{-1}(N-1)$ factor, together with population-average of NS. While the average number of trade partnerships is very high and slightly increases over the years, their average intensity is rather low (at least as compared to NS conceivable range, i.e. $[0, N-1]$) and tends to decline [69]. As far as ANND/ANNS, clustering and centrality are concerned, a more meaningful statistical assessment of the actual magnitude of empirical population-average statistics requires comparing them with expected values computed after reshuffling links and/or weights. In what follows, we consider two reshuffling schemes (RSs). For binary statistics, we compute expected values after reshuffling existing links by keeping fixed the observed density d^t (hereafter, B-RS). For weighted ones, we keep fixed the observed adjacency matrix A^t and re-distribute weights at random by reshuffling the empirical link-weight distribution $w^t = \{w_{ij}^t, i \neq j = 1, \ldots, N\}$ (hereafter, W-RS) [70]. Figure 9 shows empirical averages vs. expected values over time. Notice that empirical averages of ANND, BCC, ANNS, WCC, and RWBC are larger than expected, meaning that the WTW is on average more clustered; features a larger nearest-neighbor connectivity, and countries are on average more central than expected in comparable random graphs.

B. Correlation Structure and Node Characteristics

To further explore the topological properties of the WTW, we turn now to examine the correlation structure existing between binary- and weighted-network statistics [71]. As expected [2–4], Figure 10 shows that the binary version of the WTW is strongly disassortative in the entire sample period. Furthermore, countries holding many trade partners do not typically form trade triangles. Conversely, the weighted WTW turns out to be a weakly disassortative network. Moreover,

countries that are intensively connected (high NS) are also more clustered (high WCC). This mismatch between binary and weighted representations can be partly rationalized by noticing that the correlation between NS and ND is positive but not very large (on average about 0.45), thus hinting to a topological structure where having more trade connections does not automatically imply to be more intensively connected to other countries in terms of total trade controlled. As to centrality, RWBC appears to be positively correlated with NS, signalling that in the WTW there is little distinction between global and local centrality.

These results can be made more statistically sound by comparing empirically-observed correlation coefficients with their expected counterparts under random schemes B-RS and W-RS (see above). It turns out that almost all empirical correlation coefficients (in every year) are in absolute value larger than the absolute value of their expected counterpart under either B-RS or W-RS. This means that the magnitude of almost all observed correlations are bigger than expected. The only exception is the ANNS-NS correlation that, albeit positive, is not significantly larger than in W-RS. This indicates that whereas the binary WTW is strongly disassortative, the weak-disassortative nature of the weighted WTW is not statistically distinguishable from what we would have observed in comparable random graphs.

Another interesting issue to explore concerns the extent to which country specific characteristics relate to network properties. We focus here on the correlation patterns between network statistics and country per capita GDP (pcGDP) in order to see whether countries with a higher income are more/less connected, central and clustered. The outcomes are very clear and tend to mimic those obtained above for the correlation structure among network statistics. As Figure 11 shows, high-income countries tend to hold more, and more intense, trade relationships and to occupy a more central position. However, they trade with few and weakly-connected partners, a pattern suggesting the presence of a sort of "rich club phenomenon" and calling for further analysis, e.g. in line with Ref. [37]. Again, all empirical correlations are in absolute values larger than their expected values under reshuffling schemes B-RS and W-RS except for the ANNS-pcGDP correlation.

The overall picture that our correlation analysis suggests is one where countries holding many trade partners and/or very intense trade relationships are also the richest and most (globally) central; typically trade with many countries, but very intensively with only a few very-connected ones; and form few, but intensive, trade clusters (triangles).

Furthermore, our correlation analysis provides further evidence to the distributional stability

argument discussed above. Indeed, we have already noticed that the first four moments of the distributions of statistics under study (ND, NS, ANNS, WCC, RWBC) display a marked stability over time. Figure 10 shows that also their correlation structure is only weakly changing during the sample period. This suggests that the whole architecture of the WTW has remained fairly stable between 1981 and 2000. To further explore the implications of this result, also in the light of the ongoing processes of internationalization and globalization, we turn now to a more in-depth analysis of the in-sample dynamics and out-of-sample evolution of WTW topological structure.

C. Within-Sample Distribution Dynamics

The foregoing evidence suggests that the shape of the distributions concerning the most important topological properties of WTW displays a rather strong stability in the 1981-2000 period. However, distributional stability does not automatically rule out the possibility that between any two consecutive time steps, say $t-\tau$ and t, a lot of shape-preserving turbulence was actually going on at the node and link level, with many countries and/or link weights moving back and forth across the quantiles of the distributions. In order to check whether this is the case or not, we have computed stochastic-kernel estimates [38, 39] for the distribution dynamics concerning node and link statistics. More formally, consider a real-valued node or link statistic X. Let $\phi^\tau(\cdot,\cdot)$ be the joint distribution of $(X^t, X^{t-\tau})$ and $\psi^\tau(\cdot)$ be the marginal distribution of $X^{t-\tau}$. We estimate the τ-year stochastic kernel, defined as the conditional density $s^\tau(x|y) = \phi^\tau(x,y)/\psi^\tau(y)$ [72].

Figures 12 and 13 present the contour plots of the estimates of the 1-year kernel density of logged NS and logged positive link-weights. Notice that the bulk of the probability mass is concentrated close to the main diagonal (displayed as a solid 45° line). Similar results are found for all other real-valued node statistics (ANNS, WCC and RWBC) also at larger time lags. The kernel density of logged positive link weights, contrary to the logged NS one, is instead extremely polarized towards the extremes of the distribution range, whereas in the middle of the range it is somewhat flatter (Figure 13). We will go back to the implications that this feature has on out-of-sample distributional evolution below.

This graphical evidence hints to a weak turbulence for the distributional dynamics of all node and link statistics under analysis. To better appreciate this point, we have estimated, for all five node statistics employed above (ND, NS, ANNS, WCC, RWBC), as well as link-weight distributions, the entries of τ-step Markov transition matrices [40], where $\tau = 1, 2, \ldots, T-1$ is the time lag. More formally, suppose that the distribution dynamics of the statistic X can be well described

using K quantile classes (QCs) in every year t (see footnote 72). Given the above stability results, we can assume that the process driving the distribution dynamics of X is stationary and can be well represented by a discrete-state Markov process defined over such K QCs. Let $n_{i,j}^{t-\tau,t}$ be the number of countries whose statistic X was in QC i in year $t-\tau$ and moved to QC j in year t. Then the statistic:

$$\hat{p}_{ij}^{\tau} = \frac{\sum_{t=\tau+1}^{T} n_{i,j}^{t-\tau,t}}{\sum_{t=2}^{T}\sum_{h=1}^{K} n_{i,h}^{t-\tau,t}} \tag{1}$$

can be shown to be the maximum likelihood estimators of the true, unobservable, τ-step transition probability p_{ij}^{τ}, i.e. the probability that X belongs to QC i at $t-\tau$ and to QC j at t [41].

In order to build a measure of persistence of distribution dynamics, we have computed for each node or link statistic X the percentage mass of probability that lies within a window of ω quantiles from the main diagonal of the estimated τ-step transition-probability matrix $\hat{P}^{\tau} = \{\hat{p}_{ij}^{\tau}\}$, defined as:

$$M_{\omega,K}^{\tau}(X) = \frac{1}{K}\sum_{h=1}^{K}\sum_{l:|l-h|\leq w}^{K} \hat{p}_{hl}^{\tau}, \tag{2}$$

where the window $\omega = 0, 1, \ldots, K-1$. For example, when $\omega = 0$, $M_{0,K}^{\tau}(X)$ boils down to the trace of $\hat{P}^{\tau}$ divided by K, whereas if $\omega = 1$, $M_{1,K}^{\tau}(X)$ is the average of all the entries in the main diagonal and those lying one entry to the right and one entry to the left of the main diagonal itself. The statistic $M_{\omega,K}^{\tau}(X) \in [0,1]$ and increases the larger the probability that a country remains in the same (or nearby) QC between $t-\tau$ and t (for any given choice of τ, w and K).

Table III shows for our main statistics (ND, NS, ANNS, WCC, RWBC) and $K = 10$, the values of $M_{\omega,K}^{\tau}(X)$ as $\tau \in \{1, 4, 7, 10\}$ and $\omega = 0, 1$ [73]. The figures strongly supports the result obtained by looking at the estimated stochastic kernels. Indeed, the entries of $\hat{P}^{\tau}$ close to the main diagonal always represent a large mass of probability, thus hinting to a distribution dynamics that in the period 1981-2000 is characterized by a rather low turbulence. For example, more than 96% of countries are characterized by node statistics that either stick to the same QC between $t-\tau$ and t, or just move to a nearby QC of the distribution. This share is often close to 99%. To better statistically evaluate the figures in Table III, we have also estimated the distribution of $M_{\omega,K}^{\tau}(X)$ under reshuffling scheme W-RS, i.e. in random graphs where we keep fixed the observed adjacency matrix A^t and we re-distribute weights at random by reshuffling the observed link-weight distribution [74]. This allows us to compute confidence intervals (at 95%) for $M_{\omega,K}^{\tau}(X)$. As reported in Table III, the empirical values are always larger than the upper bound of these

confidence intervals, thus confirming the relatively strong persistence found in WTW node-statistic dynamics.

The same analysis can be also applied to the link-weight distribution $w^t = \{w^t_{ij}, i \neq j = 1, \ldots, N\}$. In order not to treat the same way existing links (with strictly positive weight) and absent links (with a zero weight), we first define the two link sets $L^t_0 = \{(i,j), i \neq j = 1, \ldots, N : w^t_{ij} = 0\}$ and $L^t_+ = \{(i,j), i \neq j = 1, \ldots, N : w^t_{ij} > 0\}$ and we then separately study the within-sample dynamics of the associated link distributions $w^t_0 = \{w^t_{ij} \in w^t : (i,j) \in L^t_0\}$ and $w^t_+ = \{w^t_{ij} \in w^t : (i,j) \in L^t_+\}$. To begin with, notice that a strong persistence also characterizes the dynamics of transition from an absent link to an existing one (and back). Indeed, the estimated probability of remaining an absent link (zero weight) is 0.9191, while that of remaining a present link (positive weight) is 0.9496. Thus, the link birth-rate is on average about 8%, while the death-rate is around 5% [75]. This means that in the period 1981-2000, the WTW has shown a slight tendency toward an increase in trade relationships. This is remarkable for two reasons. First, our panel of countries has been balanced in order to focus on a fixed number of nodes. Second, the density of the network was already very high at the beginning. Table IV shows instead the persistence measure $M^{\tau}_{\omega,K}(X)$ where X are the distributions of positive link-weights w^t_+ and the number of QCs is set to $K = 20$. Again, most of transitions occur within the same or nearby QCs, signaling that also the dynamics of weight distributions of existing links is rather persistent. Furthermore, as happens for node statistics, also in this case confidence intervals (at 95%) for randomly-reshuffled weights always lie to the left of the observed value of M. Very similar results are obtained computing the persistence measure M to logged link-weight distributions.

D. Country-Ranking Dynamics

The distributional-stability results obtained in the foregoing sections naturally hint to the emergence of a lot of stickiness in country rankings (in terms of node statistics) as well. To explore this issue, for each year $t = 1981, \ldots 2000$ we have ranked our $N = 159$ countries according to any of the five main statistics employed so far (ND, NS, ANNS, WCC, RWBC) in a descending order. The first question we are interested in is assessing to which extent also these rankings are sticky across time. We check stability of rankings by computing the time-average of Spearman rank-correlation coefficients (SRCC) [42, 43] between consecutive years [76]. More formally, let $r^t_{(i)}(X)$ be the rank of country $i = 1, \ldots, N$ in year t according to statistic X, and $\rho_{t-1,t}(X)$ be the SRCC between rankings at two consecutive years $t-1$ and t, for $t = 2, \ldots, T$. Our ranking-stability

index (RSI) for the statistic X is defined as

$$RSI(X) = \frac{1}{T-1}\sum_{t=2}^{T}\rho_{t-1,t}(X). \tag{3}$$

Of course $RSI(X) \in [-1,1]$, where $RSI(X) = -1$ implies the highest ranking turbulence, whereas $RSI(X) = 1$ indicates complete stability. The results for the WTW suggest that even rankings are very stable over time. Indeed, one has that $RSI(ND) = 0.9833$, $RSI(NS) = 0.9964$, $RSI(ANNS) = 0.9781$, $RSI(WCC) = 0.9851$ and $RSI(RWBC) = 0.9920$. Notice that, since $\rho_{t-1,t}(X) \to N(0, N^{-1})$, our $RSI(X)$ should tend to a $N(0, [N(T-1)]^{-1}) \cong N(0, 3.3102E-4)$. Therefore, our empirical values are more than 50 standard deviations to the right of 0 (no average rank correlation).

The second issue that deserves a closer look concerns detecting which countries rank high according to different statistics. Table V displays the top-20 countries in each given ranking in 2000, which, given the stability results above, well represents the entire sample period. First note that, apart from ANNS, all "usual suspects" occupy the top-ten positions. Germany scores very high for all statistics but ANNS, while the U.S. and Japan are characterized by a very high rank for weighted statistics but not for ND. This implies that they have relatively less trade partners but the share of trade that they control, the capacity to cluster, and their centrality is very high. Conversely, countries like Switzerland, Italy and Australia have a more diversified portfolio of trade partners with which they maintain less intense trade relationships. Furthermore, it is worth noting that China was already very central in the WTW in 2000, despite its clustering level was relatively lower. India was instead not present among the top-20 countries as far as NS and WCC were concerned; it was only 14th according to centrality and 11th in the ND ranking. Finally, notice how all top-20 countries in the ANNS are micro economies: they typically feature a very low NS and ND, but only tend connect to the hubs of the WTW.

Notwithstanding the presence of a relatively high ranking stability, there are indeed examples of countries moving up or falling behind over the period 1981-2000. For example, as far as centrality is concerned, Russia has steadily fallen in the RWBC ranking from the 6th to the 22th position. A similar downward pattern has been followed by Indonesia (from 17th to 36th). South Africa has instead fallen from 23th (in 1981) to 32th (in 1990) and then has become gradually more central (16th in 2000). On the contrary, the majority of high-performing Asian economies (HPAE), have been gaining positions in the RWBC ranking. For example, South Korea went from the 24th to the 8th position; Malaysia from the 43th to the 21th; Thailand started from the 42th position in 1981

and managed to become the 18th best central country in 2000. This evidence strongly contrast with the recent experience of Latin American (LATAM) economies (e.g., Mexico and Venezuela) that have – at best – maintained their position in the ranking of centrality [44].

E. Within-Sample Autocorrelation Structure and Growth Dynamics

To further explore the properties of within-sample distribution dynamics, we now investigate autocorrelation structure and growth dynamics of node and link statistics. More precisely, let X_i^t the observation of statistic X for node or link i at time t, where $i = 1, \ldots, I$, $t = 1, \ldots, T$, and I stands either for N (in case of a node statistic) or for $N(N-1)/2$ (in case of link weights). We first compute the (node or link) distribution of first-order autocorrelation coefficients (ACC) defined as:

$$\hat{r}_i(X) = \frac{\sum_{t=2}^{T} (X_i^t - \bar{X}_i^0)(X_i^{t-1} - \bar{X}_i^1)}{\sqrt{\sum_{t=2}^{T} (X_i^t - \bar{X}_i^0)^2 \sum_{t=2}^{T} (X_i^{t-1} - \bar{X}_i^1)^2}} \tag{4}$$

where $\bar{X}_i^j = (T-1)^{-1} \sum_{t=2}^{T} X_i^{t-j}$, $j = 0, 1$.

Second, we compute the first-order ACC $\hat{r}(X)$ on the (node or link) distribution of X pooled across years. To do so, we preliminary standardize the distributions $\{X_i^t, i = 1, \ldots, I\}$ for each t, so as to have zero-mean and unitary standard deviation in each year, and then we pool all T year-distributions together [77].

The left part of Table VI shows the values of $\hat{r}(X)$ together with the population mean and standard deviation of $\hat{r}_i(X)$ for our five node statistics and link weights. We also report the percentage of observations (nodes or links) for which the ACC $\hat{r}_i(X)$ turns out to be larger than zero. Both $\hat{r}(X)$ and the percentage of positive-ACF observations indicate a relatively strong persistence in the dynamics of both node and link statistics.

Given that the pooled ACC figures are very close to unity, we further check whether autoregressive dynamics governing the evolution of logged network statistics is close to a random-walk. In particular, we test whether a Gibrat dynamics (i.e., a multiplicative process on the levels X_i^t, where rates of growth of X_i^t are independent on X_i^t) applies to our variables or not [45, 46]. Notice that, under a Gibrat dynamics, X_i^t should be in the limit log-normally distributed, which is what we actually observe in our sample for the majority of node statistics (see Section III A). More formally, we begin by fitting the simple model:

$$\Delta log(X_i^t) = \beta_i log(X_i^{t-1}) + \epsilon_i^t, \tag{5}$$

where $\Delta log(X_i^t) = log(X_i^t) - log(X_i^{t-1})$ is the rate of growth of X_i^t and ϵ_i^t are white-noise errors orthogonal to $log(X_i^{t-1})$. If a Gibrat dynamics applies for a given node or link, then $\beta_i = 0$. We also fit the model in (5) to the time-pooled sample by setting $\beta_i = \beta$, where again we first standardize in each year our variables in order to wash away trends and spurious dynamics.

As the right part of Table VI shows, our data reject the hypothesis that network statistics follow a Gibrat dynamics. Indeed, both the population average of $\hat{\beta}_i$ and the pooled-sample estimate $\hat{\beta}$ are significantly smaller than zero, thus implying a process where small-valued entities (i.e., nodes and links characterized by small values of any given statistic) tend to grow relatively more than large-valued ones. This is further confirmed by the percentage of nodes or links for which $\hat{\beta}_i$ turns out to be significantly smaller than zero.

Rejection of a Gibrat dynamics also implies that the distributions of growth rates $\Delta log(X_i^t)$ should depart from Gaussian ones [47]. This is confirmed by all our pooled fits. Indeed, as Figure 14 shows for node statistics, pooled growth-rate distributions are well proxied by Laplace (fat-tailed, symmetric) densities. Furthermore, the pooled distribution of growth rates g for positive link weights is nicely described by an *asymmetric exponential power* (AEP) density [48]:

$$d(g; a_l, a_r, b_l, b_r, m) = \begin{cases} \Upsilon^{-1} e^{-\frac{1}{b_l}|\frac{g-m}{a_l}|^{b_l}}, & g < m \\ \Upsilon^{-1} e^{-\frac{1}{b_r}|\frac{g-m}{a_r}|^{b_r}}, & g \geq m \end{cases}, \tag{6}$$

where $\Upsilon = a_l b_l^{1/b_l} \Gamma(1 + 1/b_l) + a_r b_r^{1/b_r} \Gamma(1 + 1/b_r)$, and Γ is the Gamma function [78]. Maximum-likelihood estimation of tail parameters indicate that link-weight growth rates display tails much fatter than Laplace ones. Moreover, the right tail is remarkably thicker than the left one (as $\hat{b}_l = 0.5026 > 0.2636 = \hat{b}_r$), see Figure 15. Therefore, link weights are characterized by a relatively much higher likelihood of large positive growth events than of negative ones. This result brings further evidence in favor or the widespread emergence of fat-tailed growth-rate distributions in economics. In fact, recent studies have discovered that Laplace (and more generally AEP) densities seem to characterize the growth processes of many economic entities, from business companies [49–52] to world-country GDP and industrial production [53].

F. Out-of-Sample Evolution

In the preceding sections, we have investigated the within-sample dynamics of the distributions of node and link statistics. Now we turn out attention to the out-of-sample (long-run) evolution of such distributions by estimating their limiting behavior. To do so, we employ kernel density estimates obtained above to compute ergodic densities, which represent the long-run tendency of the distributions under study [79].

As already noted above, stochastic kernels of all node statistics are quite concentrated and evenly distributed along the 45° line. Therefore, it is no surprising that also their limiting distributions look quite similar to the ones in year 1981. This can be seen in Figure 16, where we exemplify this point by plotting initial vs. estimates of the ergodic distribution for the logs of NS. Both distributions present a similar shape. If any, the ergodic one exhibits a larger variability, a shift to the left of the lower tail and a shift to the right of the upper tail. This can be explained by noticing that the kernel density estimate (Figure 12) shows a relatively larger probability mass under the main diagonal in the bottom-left part of the plot, whereas in the top-right part this mass was shifted above the main diagonal. Such shape-preserving shifts hold also for the other node statistics under analysis. In particular, the ergodic distribution for node RWBC roughly preserves its power-law shape, as well as its scale exponent.

On the contrary, the shape of the stochastic kernel for logged link weights hinted at a concentration of transition densities at the extremes of the range. Middle-range values presented instead a flatter and more dispersed landscape. This partly explains why we observe a radical difference between initial and ergodic distributions of logged link weights. Whereas the initial one is close to a Gaussian (i.e., link weights are well-proxied by a log-normal density), the ergodic distribution displays a power-law shape with very small exponent. This can be seen in Figure 17, where the two plots have been superimposed.

These findings imply that the architecture of the WTW will probably evolve in such a way to undergo a re-organization of link weights (i.e., country total trade volumes) that is nevertheless able to keep unchanged the most important node topological properties. Such a re-organization seems to imply a polarization of link weights into a large majority of links carrying moderate trade flows and a small bulk of very intense trade linkages. The power-law shape of the ergodic distribution suggests that such a polarization is much more marked than at the beginning of the sample period, when the distribution of link weights was well proxied by a log-normal density. Furthermore, it must be noted that results on Gibrat dynamics in Section III E indicate that

some catching-up between low- and high-intensity links is going on within our sample period. The findings on out-of-sample evolution discussed here, on the contrary, seem to imply that such a catching-up dynamics is not so strong to lead to some convergence between e.g. low-intensity and high-intensity link weights.

G. Robustness to Alternative Weighting Schemes

All results obtained so far refer to a particular weighting procedure. To recall, the weight of a link from i to j is, after symmetrization, proportional to the total trade (imports plus exports) flowing through that link in a given year. This baseline weighting scheme is very common in the literature [1, 6–8], but treats the same way all countries irrespective of their economic importance. Are our findings robust to alternative weighting schemes? To address this issue, we have considered here two alternative economically-meaningful setups, where we wash away size effects by scaling directed link weights with the GDP of either the exporter or the importer country.

More formally, in the first alternative setup, each directed link from node i to j is now weighted by total exports of country i to country j and then divided by the country i's GDP (i.e., the *exporter* country). Such a weighting setup allows one to measure how much economy i depends on economy j as a buyer. In the second setup, we still remove size effects from trade flows, but we now divide by the GDP of the *importer* country (j's GDP). This allows us to appreciate how much economy i depends on j as a seller [80].

All our main results turn out to be quite robust to these two alternatives. This is an important point, as a weighted network analysis might in principle be sensible to the particular choice of the weighting procedure. To illustrate this point, we first compare the symmetry index for the three weighting schemes across the years, cf. Figure 18. If one scales exports by exporter's or importer's GDP the symmetry index still remains very low and close to the one found in the baseline weighting scheme. This indicates that under all three schemes an undirected-network analysis is appropriate. As a further illustration, Figure 19 reports the quantile-quantile plots of logged link-weight, GDP-scaled, distributions vs. baseline logged link weights in year 2000. It is easy to see that both alternative link-weight distributions are very similar to the baseline one. This results holds also for pooled distributions, as well as for node statistics ones. Finally, Figure 20 depicts some examples of the across-time correlation patterns between node statistics and pcGDP. Left panels refer to the first alternative weighting scheme (exports scaled by exporter GDP) whereas right panels shows what happens under the second alternative setup (exports scaled

by importer GDP). All previous results (see Figures 10 and 11) are confirmed. Notice that GDP scaling results in weaker but still significantly different from zero correlation coefficients (especially for WCC-NS). Of course, we do not expect our results to hold irrespective of *any* weighting scheme to be adopted. In fact, the binary characterization of the WTW, where some of the weighted-network results are reversed, is itself a particular weighting scheme, one that assigns to each existing link the same weight [81].

IV. CONCLUSIONS

In this paper we have explored, from a purely descriptive perspective, the within-sample dynamics and out-of-sample evolution of some key node and link statistic distributions characterizing the topological properties of the web of import-export relationships among world countries (WTW). By employing a weighted-network approach, we have shown that WTW countries holding many trade partners (and/or very intense trade relationships) are also the richest and most (globally) central; typically trade with many partners, but very intensively with only a few of them (which turn out to be themselves very connected); and form few but intensive-trade clusters. All the distributions and country rankings of network statistics display a rather strong within-sample stationarity. Our econometric tests show that node and link statistics are strongly persistent. However, Gibrat-like dynamics are rejected. This is confirmed also by the fact that the growth-rate distributions of our statistics can be well approximated by fat-tailed Laplace or asymmetric exponential-power densities. Furthermore, whereas the estimated ergodic distributions of all node-statistics are quite similar to the initial ones, the (positive) link-weight distribution is shifting from a log-normal to a power law. This suggests that a polarization between a large majority of weak-trade links and a minority of very intense-trade ones is gradually emerging in the WTW. Interestingly, such a process is likely to take place without dramatically changing the topological properties of the network.

Many extensions to the present work can be conceived. First, building on Refs. [3, 6], one may try to explore simple but economically-meaningful models of WTW dynamics that are able to reproduce the main stylized fact put forth by our purely empirical analysis. Second, one would like to explore in more details the topological properties of the WTW, both cross-sectionally and over time. Interesting questions here concern the role of geographical proximity in shaping the structure of international trade, the degree of fragility of the network, and so on. More specifically, trade flows could be disaggregated across product classes to explore how trade composition affects

network properties.

Second, one could abstract from aggregate statistical properties and analyze at a finer level the role of single countries in the network structure. For instance, how does the dynamics of degree, strength, clustering, etc. behave for single relevant countries in different regions? Do country-specific network indicators display the same time-stationarity of their aggregate counterparts?

Finally, in line with Ref. [54], one can ask whether node statistics characterizing connectivity, clustering, centrality and so on, can be employed as explanatory variables for the dynamics of country growth rates and development patterns.

---

[1] X. Li, Y. Y. Jin, and G. Chen, Physica A: Statistical Mechanics and its Applications **328**, 287 (2003).

[2] A. Serrano and M. Boguñá, Physical Review E **68**, 015101(R) (2003).

[3] D. Garlaschelli and M. Loffredo, Physical Review Letters **93**, 188701 (2004).

[4] D. Garlaschelli and M. Loffredo, Physica A **355**, 138 (2005).

[5] A. Serrano, M. Boguñá, and A. Vespignani, Journal of Economic Interaction and Coordination **2**, 111 (2007).

[6] K. Bhattacharya, G. Mukherjee, J. Sarämaki, K. Kaski, and S. Manna, arXiv:0707.4343v1 (2007).

[7] K. Bhattacharya, G. Mukherjee, and S. Manna, arXiv:0707.4347v1 (2007).

[8] D. Garlaschelli, T. D. Matteo, T. Aste, G. Caldarelli, and M. Loffredo, The European Physical Journal B **57**, 1434 (2007).

[9] G. Fagiolo, Physical Review E **76**, 026107 (2007).

[10] G. Fagiolo, J. Reyes, and S. Schiavo, LEM Working Paper 2007-16, Sant'Anna School of Advanced Studies (2007).

[11] I. Tzekina, K. Danthi, and D. Rckmore, arXiv:0709.2630v1 (2007).

[12] G. Fagiolo, S. Schiavo, and J. Reyes, Physica A **387**, 3868 (2008).

[13] J. Stiglitz, *Globalization and its discontents* (Penguin, London, 2002).

[14] A. Dreher, N. Gaston, and P. Martens, *Measuring Globalisation: Gauging Its Consequences* (Springer, Berlin, 2008).

[15] P. Krugman, Brookings Papers on Economic Activity **26**, 327 (1995).

[16] J. F. Helliwell and T. Padmore, in *Handbook of International Economies*, edited by R. Jones and

P. Kenen (Elsevier Science Publishers B.V., 1985).

[17] M. Artis, A. Beatriz, C. Galvão, and M. Marcellino, Economics Working Papers ECO2003/18, European University Institute (2003).

[18] K. Forbes, in *Preventing Currency Crises in Emerging Markets*, edited by S. Edwards and J. Frankel (Chicago, University of Cicago Press, 2002).

[19] T. Abeysinghe and K. Forbes, Review of International Economics **13**, 356 (2005).

[20] R. Albert and A.-L. Barabási, Rev. Mod. Phys. **74**, 47 (2002).

[21] S. Dorogovtsev and J. Mendes, *Evolution of Networks: From Biological Nets to the Internet and WWW* (Oxford, Oxford University Press, 2003).

[22] M. Newman, SIAM Review **45**, 167 (2003).

[23] R. Pastos-Satorras and A. Vespignani, *Evolution and Structure of the Internet* (Cambridge, Cambridge University Press, 2004).

[24] A. Barrat, M. Barthélemy, R. Pastor-Satorras, and A. Vespignani, Proceedings of the National Academy of Sciences **101**, 3747 (2004).

[25] A. Barrat, M. Barthélemy, and A. Vespignani, arXiv:cond–mat/0401057v2 (2005).

[26] M. Barthélemy, A. Barrat, R. Pastor-Satorras, and A. Vespignani, Physica A **346**, 34 (2005).

[27] M. Newman, The European Physical Journal B **38**, 321 (2004).

[28] K. Gleditsch, Journal of Conflict Resolution **46**, 712 (2002), data available on-line at http://privatewww.essex.ac.uk/∼ksg/data.html.

[29] G. Fagiolo, Economics Bulletin **3**, 1 (2006), available on-line at http://economicsbulletin. vanderbilt.edu/ 2006/volume3/ EB–06Z10134A.pdf.

[30] R. Pastor-Satorras, Vázquez, and A. Vespignani, Physical Review Letters **87**, 258701 (2001).

[31] A. DeMontis, M. Barthélemy, A. Chessa, and A. Vespignani, arXiv:physics/0507106v2 (2005).

[32] J. Saramaki, M. Kivelä, J. Onnela, K. Kaski, and J. Kertész, Phsycial Review E **75**, 027105 (2007).

[33] D. Watts and S. Strogatz, Nature **393**, 440 (1998).

[34] M. Newman, Social Networks **27**, 39 (2005).

[35] E. Fisher and F. Vega-Redondo, Working Paper, Cal Poly (2006).

[36] J. Scott, *Social Network Analysis: A Handbook* (London, Sage, 2000).

[37] M. A. Serrano, arXiv/0802.3122v2 (2008).

[38] K. L. Chung, *Markov Chains with Stationary Transition Probabilities* (Springer-Verlag, Berlin, 1960).

[39] C. Futia, Econometrica **50**, 377 (1982).

[40] A. Stuart and K. Ord, *Kendalls Advanced Theory of Statistics*, vol. I (Edward Arnold, London, 1994), 6th ed.

[41] T. Anderson and A. Goodman, The Annals of Mathematical Statistics **28**, 89 (1957).

[42] C. Spearman, American Journal of Psychology **15**, 72101 (1904).

[43] M. Hollander and D. Wolfe, *Nonparametric statistical methods* (Wiley: New York, 1973).

[44] J. Reyes, G. Fagiolo, and S. Schiavo, LEM Working Paper 2008-10, Sant'Anna School of Advanced Studies (2008).

[45] R. Gibrat, *Les Inégalités Economiques* (Librairie du Recueil Sirey: New York, 1931).

[46] J. Sutton, Journal of Economic Literature **35**, 40 (1997).

[47] G. Bottazzi and A. Secchi, RAND Journal of Economics **37**, 235 (2006).

[48] G. Bottazzi and A. Secchi, Working Paper 2006/19, Laboratory of Economics and Management (LEM), Sant'Anna School of Advanced Studies, Pisa, Italy (2006).

[49] M. Stanley, L. Amaral, S. Buldyrev, S. Havlin, H. Leschhorn, P. Maass, M. Salinger, and H. Stanley, Nature **379**, 804 (1996).

[50] L. Amaral, S. Buldyrev, S. Havlin, M. Salinger, H. Stanley, and M. Stanley, Physica A **244**, 1 (1997).

[51] D. Canning, L. Amaral, Y. Lee, M. Meyer, and H. Stanley, Economic Letters **60**, 335 (1998).

[52] D. Fu, F. Pammolli, S. Buldyrev, M. Riccaboni, K. Matia, K. Yamasaki, and H. Stanley, Proceedings of the Nationaly Academy of Science **102**, 18801 (2005).

[53] G. Fagiolo, M. Napoletano, and A. Roventini, Journal of Applied Econometrics (2007), forthcoming.

[54] R. Kali and J. Reyes, Journal of International Business Studies **38**, 595 (2007).

[55] A. Bera and C. Jarque, Economics Letters **6**, 255 (1980).

[56] A. Bera and C. Jarque, Economics Letters **7**, 313 (1981).

[57] B. Bollobás, *Random Graphs* (New York, Academic Press, 1985).

[58] S. N. Durlauf and D. T. Quah, in *Handbook of Macroeconomics*, edited by J. B. Taylor and M. Woodford (Elsevier, 1999), vol. 1, chap. 4, pp. 235–308.

[59] D. Fiaschi and M. Lavezzi, Journal of Development Economics **84**, 271 (2007).

[60] A. Fuliński, Z. Grzywna, I. Mellor, Z. Siwy, and P. N. R. Usherwood, Phys. Rev. E **58**, 919 (1998).

[61] For example, "openness to trade" of a given country is traditionally measured by the ratio of exports plus imports to country's gross domestic product (GDP).

[62] That is, they weight each bilateral trade relation by the difference between exports and imports. Notice that, as happens also in Refs. [6, 7], their across-year comparison may be biased by the fact

that trade flows are expressed in current U.S. dollars and do not appear to be properly deflated.

[63] In Section III G we explore what happens if we employ a few alternative definitions for link weights.

[64] The expected value of the statistic in a random graph where link weights are uniformly and independently distributed as a uniform in the unit interval is 0.5 [29]. Furthermore, the expected value computed by randomly reshuffling in each year the empirically-observed weights among existing links ranges in the same period from 0.0230 to 0.0410. Therefore, the empirical value is significantly smaller than expected.

[65] Cf. Ref. [32] for alternative definitions of the clustering coefficient for weighted undirected networks. Here we employ the above formulation because it is the only one retaining two properties important to fully characterize clustering in trade networks, namely (i) WCC_i^t takes into account the weight of all links in any given triangle; (ii) WCC_i^t is invariant to weight permutations in one triangle.

[66] Notice that the fraction of strictly positive links (over all possible links) also defines network density. More on that below.

[67] More formally, let X_i^t be the value of the node statistic X at time t for country i and $M^k(\cdot)$ the moment operator that for $k = 1, 2, 3, 4$ returns respectively the mean, standard deviation, skewness and kurtosis. The time-average of absolute-valued 1-year growth rates of the k-th moment-statistic is defined as $\frac{1}{T-1}\sum_{t=2}^{T}|(E^k(X_i^t)/E^k(X_i^{t-1})-1)|$.

[68] Table II reports p-values for the Jarque-Bera test [55, 56], the null hypothesis being that the logs of positive-valued statistics are normally distributed with unknown parameters. Alternative normality tests (Lilliefors, Anderson-Darling, etc.) yield similar results.

[69] At the extreme, if in every year t the network were an Erdös-Renyi random-graph [57] with link probability equal to network density d^t and link weights drawn from an i.i.d. uniform r.v. defined on the unit interval (U[0,1]) – uniformly weighted ER graph henceforth – the expected NS would have been $\frac{1}{2}(N-1)[d^t]^2$, that is a value ranging over time between 22.9079 and 32.7699.

[70] Notice that under if the network were an uniformly weighted ER graph (see above), one would have obtained $E(ANND_i^t) = 1 + (N-2)d^t$, $E(ANNS_i^t) = E(NS_i^t) = \frac{N-2}{2}(d^t)^2$, $E(BCC_i^t) = d^t$ and $E(WCC_i^t) = \frac{27}{64}d^t$; see [9].

[71] More precisely, the correlation coefficient between two variables X and Y is defined here as the product-moment (Spearman) sample correlation, i.e. $\sum_i (x_i - \overline{x})(y_i - \overline{y})/[(N-1)s_X s_Y]$, where $\overline{x}$ and $\overline{y}$ are sample averages and s_X and s_Y are sample standard deviations.

[72] Cf. Refs. [58, 59] for economic applications. Here and in what follows, Markovianity of the statistics

under analysis has been assumed without performing more rigorous statistical tests [60]. This is actually one of the next points in our agenda.

[73] Parameters outside these ranges and choices do not change the main implications of the analysis. Similar results also are obtained if one computes the statistic $M^{\tau}_{\omega,K}$ on logged distributions of X (i.e., logs of node statistics and positive link weights) and/or one preliminary re-scales the data by removing the time-averages of the distributions in order to wash away possible trends.

[74] The distributions of $M^{\tau}_{\omega,K}(X)$ turn out to be well-proxied by Gaussian densities.

[75] Standard deviations of such estimates are quite small. Let $\hat{p}_{00}$ and $\hat{p}_{++}$, respectively, be the probability of remaining a zero and positive link weight. We find that $\sigma(\hat{p}_{00}) = 0.0034$ and $\sigma(\hat{p}_{++}) = 0.0023$. Similarly, let $\hat{p}_{0+}$ and $\hat{p}_{+0}$ be the probability of becoming a positive (respectively, zero) link weight. Since $\hat{p}_{00} = 1 - \hat{p}_{0+}$ and $\hat{p}_{++} = 1 - \hat{p}_{+0}$ by construction, then $\sigma(\hat{p}_{0+}) = \sigma(\hat{p}_{00})$ and $\sigma(\hat{p}_{+0}) = \sigma(\hat{p}_{++})$.

[76] We focus here only on one-year lags between rankings. An interesting extension to the present analysis would be to check for stability of rankings across time lags of length $\tau > 1$.

[77] We stop at first-order autocorrelation coefficients because of the few time observations available. Notwithstanding their low statistical significance, also second-order ACCs turn out to be positive albeit much smaller than first-order ones.

[78] The AEP features five parameters. The parameter m controls for location. The two a's parameters control for scale to the left (a_l) and to the right (a_r) of m. Larger values for a's imply – *coeteris paribus* – a larger variability. Finally, the two b's parameters govern the left (b_l) and right (b_l) tail behavior of the distribution. To illustrate this point, let us start with the case of a symmetric exponential power (EP), i.e. when $a_l = a_r = a$ and $b_l = b_r = b$. It is easy to check that if $b = 2$, the EP boils down to the normal distribution. In that case, the correspondent HCE distribution would be log-normal. If $b < 2$, the EP displays tails thicker than a normal one, but still not heavy. In fact, for $b < 2$, the EP configures itself as a medium-tailed distribution, for which all moments exist. In the case $b = 1$ we recover the Laplace distribution. Finally, for $b > 2$ the EP features tails thinner than a normal one and still exponential.

[79] Given the real-valued statistic X, its ergodic distribution $\phi_{\infty}(\cdot)$ is implicitly defined for any given τ as $\phi_{\infty}(x) = \int s^{\tau}(x|z)\phi_{\infty}(z)dz$, where $s^{\tau}(x|z)$ is the stochastic kernel defined in Section III C. See also Ref. [58].

[80] We have also experimented with the weighting scheme where trade is scaled *by the sum* of importer's and exporter's GDPs without detecting any significant difference.

[81] In this respect, an interesting exercise would imply to find (if any) a proper re-scaling or manipulation of original trade flows that makes weighted and binary results looking the same.

	Average Absolute Growth Rates			
	Mean	Std Dev	Skewness	Kurtosis
ND	0.0143	0.0047	0.0375	0.0086
ANND	0.0079	0.0279	0.0116	0.0260
BCC	0.0043	0.0197	0.0615	0.0205
NS	0.0379	0.0412	0.0263	0.0317
ANNS	0.0479	0.0512	0.0223	0.0452
WCC	0.0544	0.0097	0.0274	0.0543
RWBC	0.0049	0.0107	0.0251	0.0556

TABLE I: Average over time of absolute-valued 1-year growth rates of the first four moments of node statistics. Given the value of the node statistic X at time t for country i (X_i^t) and $M^k(\cdot)$ the moment operator that for $k = 1, 2, 3, 4$ returns respectively the mean, standard deviation, skewness and kurtosis, the time-average of absolute-valued 1-year growth rates of the k-th moment-statistic is defined as $\frac{1}{T-1}\sum_{t=2}^{T}|(E^k(X_i^t)/E^k(X_i^{t-1}) - 1)|$.

	1981	1982	1983	1984	1985	1986	1987	1988	1989	1990
ND	0.0000***	0.0000***	0.0010***	0.0000***	0.0000***	0.0000***	0.0010***	0.0000***	0.0010***	0.0000***
ANND	0.0277**	0.0261**	0.0400**	0.0403**	0.0525*	0.0309**	0.0333**	0.0197**	0.1254	0.1020
BCC	0.0060***	0.0040***	0.0040***	0.0040***	0.0050***	0.0020***	0.0050***	0.0030***	0.0080***	0.0040***
NS	0.2925	0.2046	0.4021	0.2870	0.4344	0.6804	0.6238	0.5300	0.3496	0.5343
ANNS	0.1118	0.2500	0.2724	0.2463	0.2816	0.2532	0.3243	0.1633	0.1666	0.1065
WCC	0.5673	0.2525	0.2821	0.2874	0.2867	0.2601	0.3564	0.2035	0.2005	0.1202
RWBC	0.0000***	0.0000***	0.0000***	0.0000***	0.0000***	0.0000***	0.0000***	0.0000***	0.0000***	0.0000***

	1991	1992	1993	1994	1995	1996	1997	1998	1999	2000
ND	0.0010***	0.0020***	0.0010***	0.0010***	0.0020***	0.0000***	0.0000***	0.0000***	0.0000***	0.0000***
ANND	0.0810*	0.0630*	0.0900*	0.0700*	0.0580*	0.0400**	0.0480**	0.0460**	0.0400**	0.0260**
BCC	0.0090***	0.0040***	0.0040***	0.0020***	0.0020***	0.0060***	0.0050***	0.0050***	0.0050***	0.0050***
NS	0.5367	0.2398	0.2917	0.2016	0.3685	0.4693	0.6000	0.6312	0.5918	0.5260
ANNS	0.2450	0.0905*	0.1402	0.1133	0.1269	0.0574*	0.0734*	0.0899*	0.0668*	0.1385
WCC	0.2661	0.1166	0.1562	0.1356	0.1358	0.0638*	0.1206	0.1095	0.1072	0.1583
RWBC	0.0000***	0.0000***	0.0000***	0.0000***	0.0000***	0.0000***	0.0000***	0.0000***	0.0000***	0.0000***

TABLE II: P-values for Jarque-Bera normality test [55, 56]. Null hypothesis: Logs of (positive-valued) distribution are normally-distributed with unknown parameters. Asterisks: (*) null hypothesis rejected at 10%; (**) null hypothesis rejected at 5%; (***) null hypothesis rejected at 1%.

$\omega = 0$	τ			
Statistic	1	4	7	10
$M^{\tau}_{\omega,K}(ND)$	0.8674	0.7794	0.7282	0.6943
$M^{\tau}_{\omega,K}(NS)$	0.9346	0.8612	0.8234	0.7874
$M^{\tau}_{\omega,K}(ANNS)$	0.8541	0.7577	0.7145	0.6656
$M^{\tau}_{\omega,K}(WCC)$	0.8553	0.7490	0.6776	0.6377
$M^{\tau}_{\omega,K}(RWBC)$	0.9004	0.8280	0.7899	0.7515
C.I. (Reshuffled)	[0.1854,0.2146]	[0.1842,0.2159]	[0.1823,0.2176]	[0.1800,0.2200]

$\omega = 1$	τ			
Statistic	1	4	7	10
$M^{\tau}_{\omega,K}(ND)$	0.9950	0.9881	0.9753	0.9640
$M^{\tau}_{\omega,K}(NS)$	0.9997	0.9965	0.9923	0.9875
$M^{\tau}_{\omega,K}(ANNS)$	0.9930	0.9835	0.9710	0.9579
$M^{\tau}_{\omega,K}(WCC)$	0.9980	0.9918	0.9787	0.9686
$M^{\tau}_{\omega,K}(RWBC)$	0.9990	0.9965	0.9952	0.9906
C.I. (Reshuffled)	[0.5020,0.5370]	[0.5004,0.5385]	[0.4981,0.5406]	[0.4954,0.5436]

TABLE III: Distribution dynamics. Persistence measure $M^{\tau}_{\omega,K}(X)$ for the distributions of node statistics and for alternative choices of the window $\omega \in \{0, 1\}$ and the time lag $\tau \in \{1, 4, 7, 10\}$. All statistics refer to $K = 10$ quantile classes. The lines labeled as "C.I. (Reshuffled)" contain confidence intervals (at 95%) for the mean of the distribution of the statistic M in random graphs where the observed adjacency matrices A^t are kept fixed and weights are re-distributed at random by reshuffling the observed link-weight distributions $w^t = \{w^t_{ij}, i \neq j = 1, \ldots, N\}$. Values of $M^{\tau}_{\omega,K}(X)$ close to one and to the right of confidence intervals indicate a strong persistence of the associated with-sample distribution dynamics.

	τ			
	1	4	7	10
$\omega = 0$	0.8116	0.7073	0.6464	0.6012
C.I. (Reshuffled)	[0.1974,0.2026]	[0.1971,0.2029]	[0.1969,0.2032]	[0.1962,0.2037]
$\omega = 1$	0.9910	0.9733	0.9562	0.9397
C.I. (Reshuffled)	[0.5175,0.5238]	[0.5172,0.5241]	[0.5170,0.5248]	[0.5167,0.5253]

TABLE IV: Distribution dynamics. Persistence measure $M^{\tau}_{\omega,K}(X)$ for the distributions of positive link weights and for alternative choices of the window $\omega \in \{0, 1\}$ and the time lag $\tau \in \{1, 4, 7, 10\}$. All statistics refer to $K = 20$ quantile classes. The lines labeled as "C.I. (Reshuffled)" contain confidence intervals (at 95%) for the mean of the distribution of the statistic M in random graphs where the observed adjacency matrices A^t are kept fixed and weights are re-distributed at random by reshuffling the observed link-weight distributions $w^t = \{w^t_{ij}, i \neq j = 1, \ldots, N\}$. Values of $M^{\tau}_{\omega,K}(X)$ close to one and to the right of confidence intervals indicate a strong persistence of the associated with-sample distribution dynamics.

Rank	ND	NS	ANNS	WCC	RWBC
1	Germany	USA	Sao Tom & Principe	USA	USA
2	Italy	Germany	Kiribati	Germany	Germany
3	UK	Japan	Nauru	Japan	Japan
4	France	France	Tonga	UK	France
5	Switzerland	China	Vanuatu	China	UK
6	Australia	UK	Tuvalu	France	China
7	Belgium	Canada	Burundi	Italy	Italy
8	Netherlands	Italy	Botswana	Netherlands	S. Korea
9	Denmark	Netherlands	Lesotho	S. Korea	Netherlands
10	Sweden	Belgium	Maldives	Singapore	Belgium
11	India	S. Korea	Solomon Islands	Mexico	Spain
12	Spain	Mexico	Bhutan	Belgium	Australia
13	USA	Taiwan	Comoros	Spain	Singapore
14	China	Singapore	Seychelles	Taiwan	India
15	Norway	Spain	Saint Lucia	Canada	Taiwan
16	Japan	Switzerland	Guinea-Bissau	Arab Emirates	S. Africa
17	Taiwan	Malaysia	Mongolia	Saudi Arabia	Brazil
18	Malaysia	Sweden	Cape Verde	Iraq	Thailand
19	Ireland	Thailand	Grenada	Switzerland	Saudi Arabia
20	Canada	Australia	Fiji	Russia	Canada

TABLE V: Country rankings in year 2000 according to node statistics.

	First-Order Autocorrelation				Gibrat-Regression Parameter			
	Mean	SD	%(> 0)	Pooled	Mean	StdDev	%(< 0)	Pooled
ND	0.6438	0.2222	0.8428	0.9859	-0.3636	0.2235	0.6667	-0.1330
NS	0.6795	0.1170	0.9623	0.9949	-0.3186	0.1176	0.7799	-0.1910
ANNS	0.6353	0.0686	0.9811	0.9539	-0.3609	0.0670	0.9811	-0.2235
WCC	0.6404	0.1414	0.9119	0.9855	-0.3596	0.1414	0.8302	-0.2866
RWBC	0.6203	0.2007	0.8050	0.9983	-0.3795	0.2007	0.7862	-0.3651
Pos Link Weights	0.4330	0.3069	0.4171	0.9940	-0.4368	0.2299	0.9196	-0.1422

TABLE VI: First-order autocorrelation coefficient $\hat{r}_i(X)$ (4) and $\hat{\beta}_i$ parameter in Gibrat regressions (5) for node and link statistics. Mean and SD columns: Population average and standard deviation computed across node or links. Columns labeled by $\%(> 0)$ or $\%(< 0)$ report the percentage of nodes or links whose estimate is larger or smaller than zero. Columns labeled by "Pooled" report estimates for the time-pooled normalized sample (i.e., the sample obtained by first standardizing each observation by the mean and standard deviation of the year, and then stacking all years in a column vector).

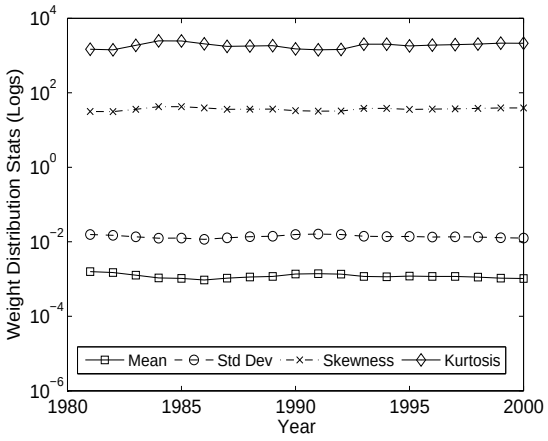


FIG. 1: Sample moments of the link-weight distribution vs. years. Log scale on Y-axis.

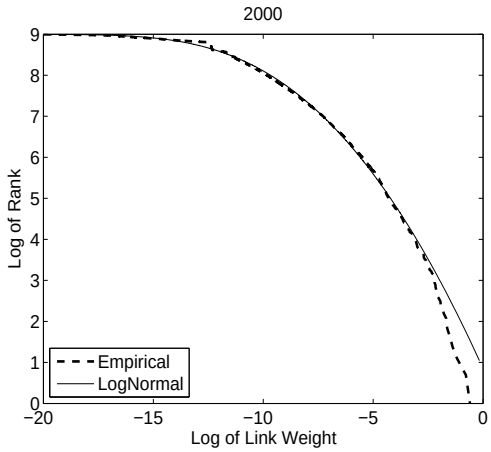


FIG. 2: Size-rank (log-log) plot of the link-weight distribution in year 2000.

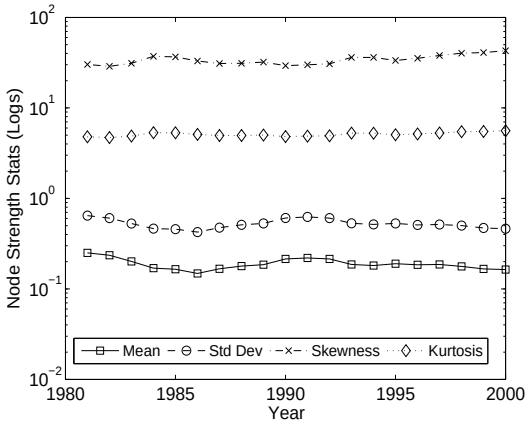


FIG. 3: Sample moments of the node strength (NS) distribution vs. years. Log scale on Y-axis.

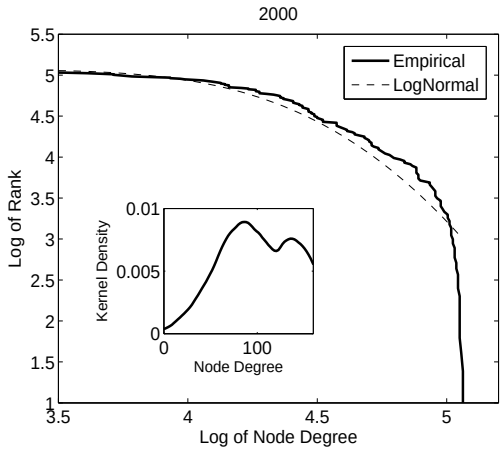


FIG. 4: Size-rank (log-log) plot of node-degree distribution in year 2000. Inset: Kernel density estimate.

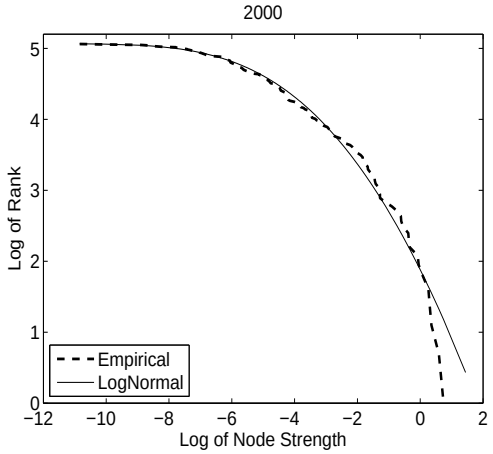


FIG. 5: Size-rank (log-log) plot of node-strength distribution in year 2000.

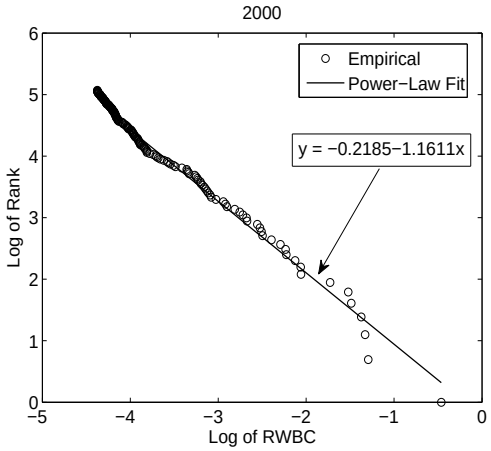


FIG. 6: Size-rank (log-log) plot of node random-walk betweenness centrality (RWBC) distribution in year 2000. Solid line: Power-law fit (equation of the regression line in the inset).

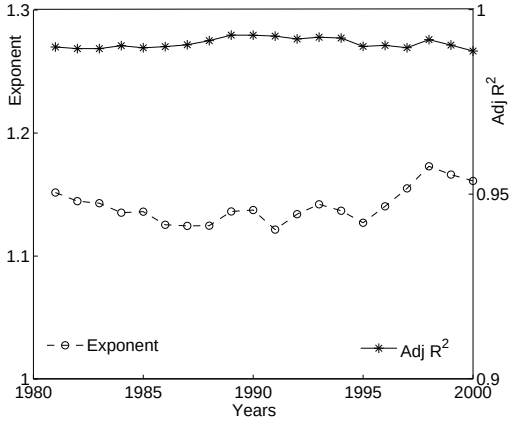


FIG. 7: Left Y-axis scale: Estimated power-law exponent for node random-walk betweenness centrality (RWBC) distributions vs. years. Right Y-axis scale: Adjusted R^2 associated to the power-law fit.

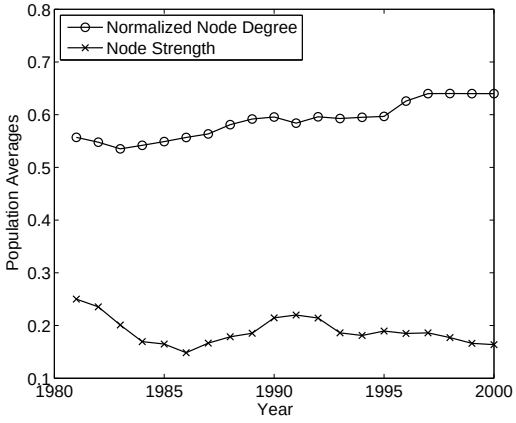


FIG. 8: Population averages of node degree normalized by population size $N = 159$ and node strength vs. years.

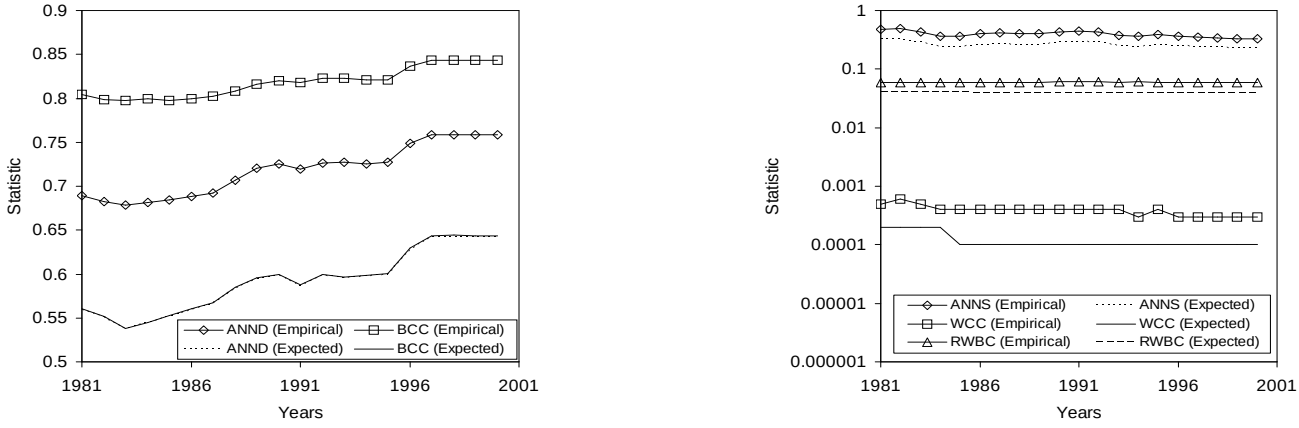


FIG. 9: Population average vs. expected values of node statistics. Expected values for binary-network statistics (left) are computed by reshuffling binary links by keeping observed density fixed. Expected values for weighted-network statistics (right) are computed by reshuffling observed link weights while keeping the binary structure fixed.

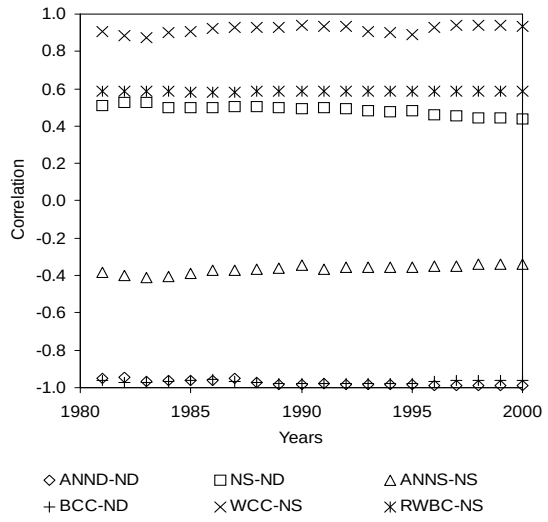


FIG. 10: Correlation between node statistics vs. years.

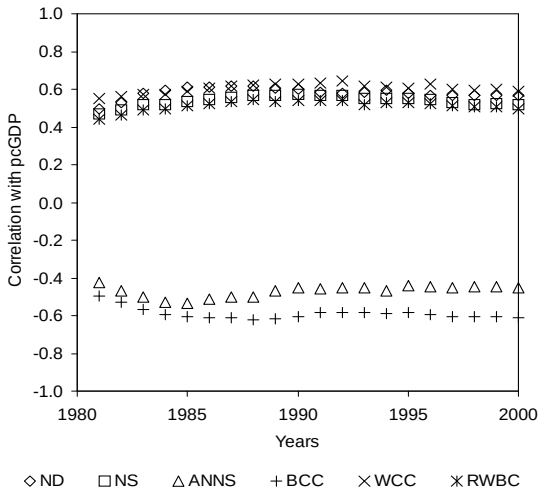


FIG. 11: Correlation between node statistics and country per-capita gross-domestic product (GDP) vs. years.

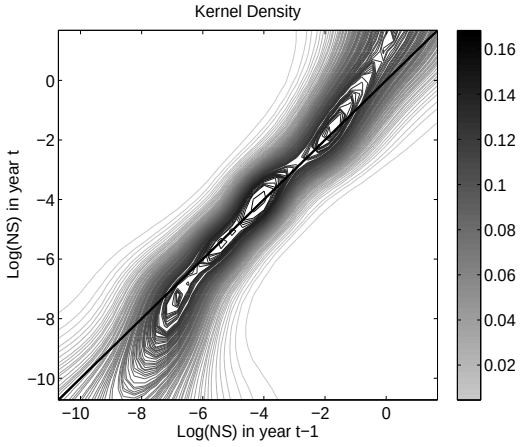


FIG. 12: Contour plot of stochastic-kernel estimates for logged node strength (NS). Solid line: Main 45° diagonal.

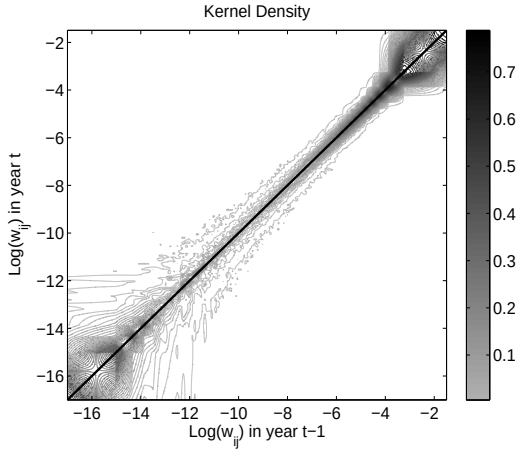


FIG. 13: Contour plot of stochastic-kernel estimates for logged positive link-weights $(\log(w_{ij}^t), w_{ij}^t > 0)$. Solid line: Main 45° diagonal.

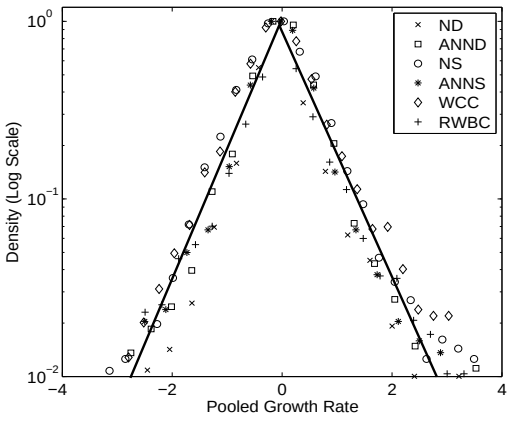


FIG. 14: Pooled growth-rate distributions for node statistics. Y-axis: Log Scale. Solid lines: Laplace fit.

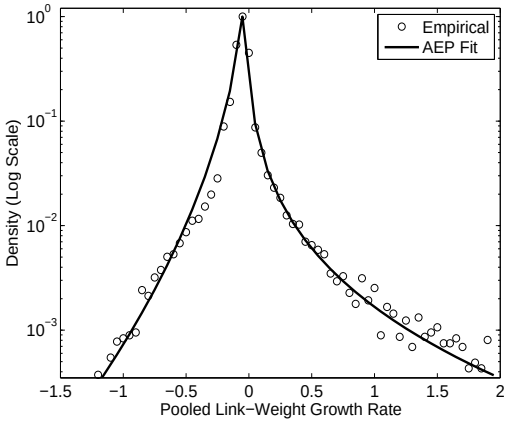


FIG. 15: Pooled growth-rate distribution of link weights. Y-axis: Log Scale. Solid lines: Asymmetric exponential-power (AEP) fit (6). Parameter estimates: $\hat{b}_l = 0.5026$, $\hat{b}_r = 0.2636$, $\hat{a}_l = 0.0511$, $\hat{a}_r = 0.0615$, $\hat{m} = -0.0202$.

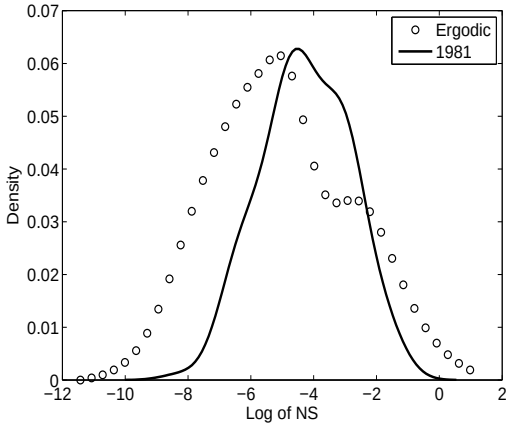


FIG. 16: Node Strength (NS): Kernel density of initial distribution (year=1981) vs. estimate of ergodic (limiting) distribution.

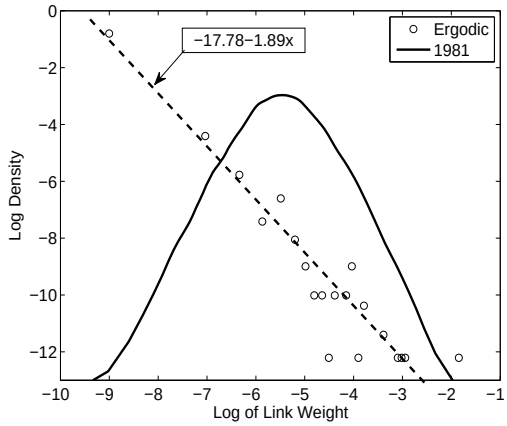


FIG. 17: Positive link weights: Kernel density of initial distribution (year=1981) vs. estimate of ergodic (limiting) distribution. Dotted line: Power-law fit (equation shown in inset). Note: Log scale on y-axis.

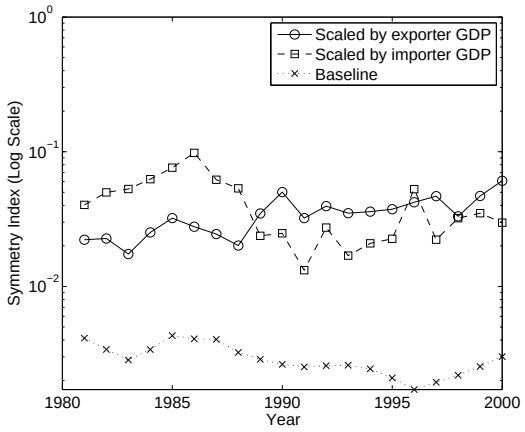


FIG. 18: Symmetry index applied to the baseline weighting scheme vs. symmetry index in the two alternative weighting schemes analyzed. First scheme: Exports scaled by exporter GDP. Second scheme: Exports scaled by importer GDP.

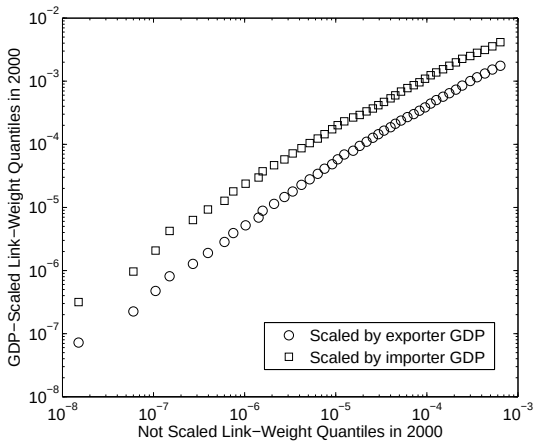


FIG. 19: Quantile-quantile plots of logged link-weight distributions in year 2000. X-axis: Quantiles of logged link-weight distribution for the baseline weighting scheme. Y-axis: Quantiles of logged link-weight distributions in the two alternative weighting schemes analyzed. First scheme: Exports scaled by exporter GDP. Second scheme: Exports scaled by importer GDP.

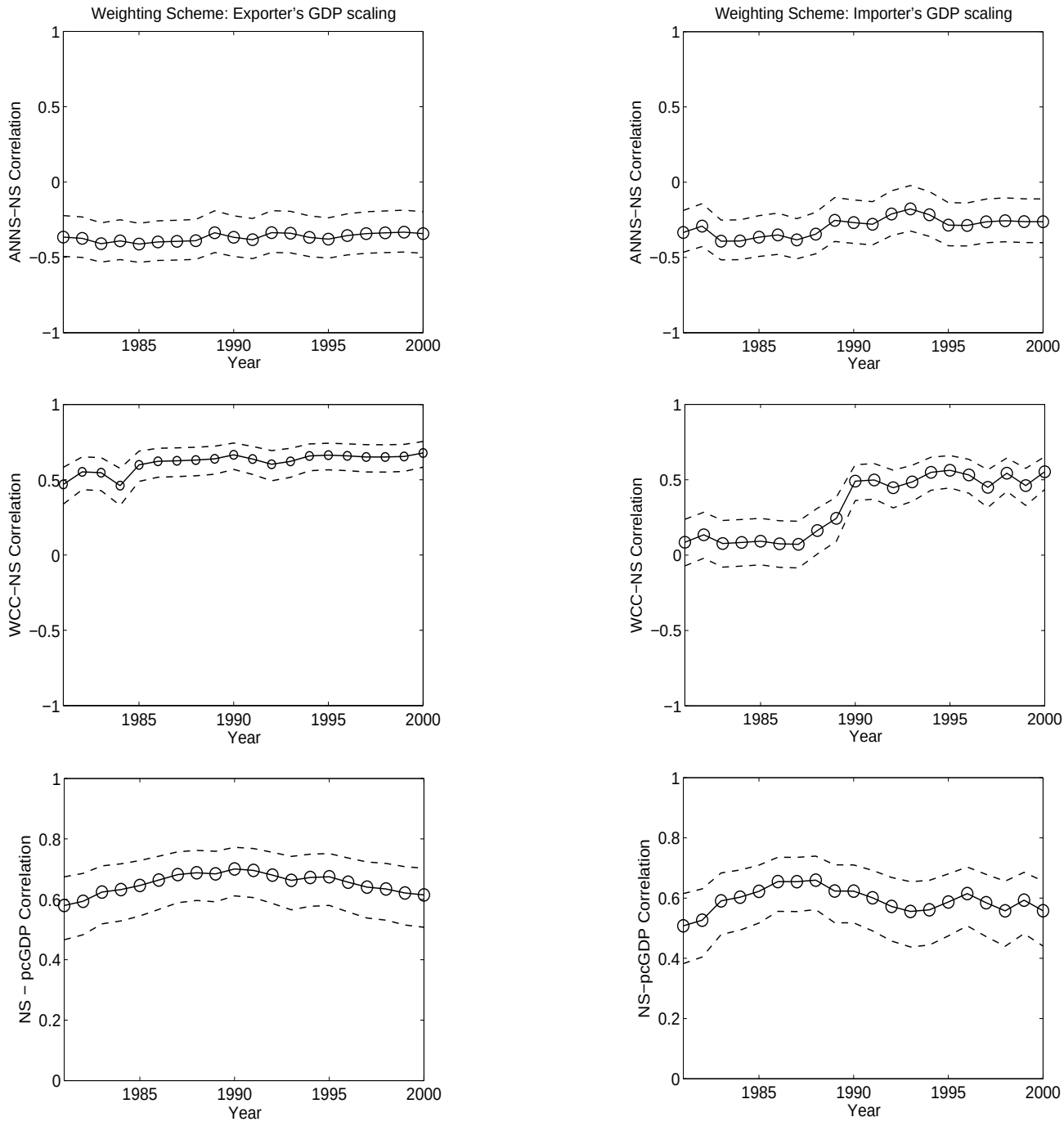


FIG. 20: Correlation structure among node statistics in the two alternative weighting schemes analyzed. Left figures: Exports scaled by exporter GDP. Right Figures: Exports scaled by importer GDP. Dotted lines: 95% confidence intervals for population averages.